Thin Solid Films 518 (2010) 5700–5703

Contents lists available at ScienceDirect

Thin Solid Films

journal homepage: www.elsevier.com/locate/tsf

Growth of 3C–SiC on Si(111) using the four-step non-cooling process

Jui-Min Liu [a], Wei-Yu Chen [a], J. Hwang [a,*], C.-F. Huang [b], Wei-Lin Wang [c], Li Chang [c]

[a] Department of Materials Science and Engineering, National Tsing Hua University, Hsin-Chu City, Taiwan, ROC
[b] Department of Electrical Engineering, National Tsing Hua University, Hsin-Chu City, Taiwan, ROC
[c] Department of Materials Science and Engineering, National Chiao Tung University, Hsin-Chu City, Taiwan, ROC

ARTICLE INFO

Available online 12 May 2010

Keywords:
Silicon carbide
Low pressure chemical vapor deposition
X-ray diffraction
Crystal microstructure

ABSTRACT

A modified four-step method was applied to grow a 3C–SiC thin film of high quality on the off-axis 1.5° Si(111) substrate in a mixed gas of C_3H_8, SiH_4 and H_2 using low pressure chemical vapor deposition. The modified four-step method adds a diffusion step after the carburization step and removes the cooling from the traditional three-step method (clean, carburization, and growth). The X-ray intensity of the 3C–SiC(111) peak is enhanced from 5×10^4 counts/s (the modified three steps) to 1.1×10^5 counts/s (the modified four steps). The better crystal quality of 3C–SiC is confirmed by the X-ray rocking curves of 3C–SiC(111). 3C–SiC is epitaxially grown on Si(111) supported by the selected area electron diffraction patterns taken at the 3C–SiC/Si(111) interface. Some {111} stacking faults and twins appear inside the 3C–SiC, which may result from the stress induced in the 3C–SiC thin film due to lattice mismatch. The diffusion step plays roles in enhancing the formation of Si–C bonds and in reducing the void density at the 3C–SiC/Si(111) interface.

1. Introduction

The growth of 3C–SiC on either Si(100) or Si(111) has attracted much attention due to both fundamental and practical reasons. The physical properties of SiC such as high thermal conductivity, high breakdown field and high saturation velocity [1,2] increase the potential for the applications of high power and high frequency electronic devices [3]. The drives to grow 3C–SiC on Si(100) or Si(111) in the past decades are due to lower production cost.

The major breakthrough of the growth of 3C–SiC on Si was achieved by Nishino and Powell in 1983 [4]. The difficulties of large lattice mismatch (~20%) and large difference in thermal expansion coefficients (~8%) between Si and SiC were partially overcome by introducing a carburization process. The carburization process is inserted before the growth of SiC using a three-step method (clean, carburization and growth). A carbon containing gas can be decomposed and to deposit amorphous carbon on Si at the carburization step such that an ultra-thin SiC film can be formed for further growth of SiC at the growth step. However, there still exist defects such as dislocations, twins, stacking faults and anti-phase boundaries near the 3C–SiC/Si interface [5–9].

The concept of carburization has been widely used by other research groups since then [10–14]. In the conventional three-step method, the full process time is long since it is required to cool the samples back to room temperature or lower temperature (e.g. ~500 °C) between each step in order to obtain good crystal quality. In 2008, Chen et al. developed the modified four-step method (clean, carburization, diffusion and growth) by inserting a diffusion step and removing the cooling step in the conventional three-step method [15]. The temperature versus time for the modified four-step method is sketched in Fig. 1. The diffusion step, after the carburization step, is performed at 1350 °C such that the formation of SiC in the as-carburized layer on Si(100) is enhanced in a short time. The quick formation of an ultra-thin SiC layer on top of Si (100) enables the formation of void-free 3C–SiC/Si(100) interface [10]. A better crystal quality of 3C–SiC can be grown on Si(100) in a mixed gas of propane (C_3H_8), silane (SiH_4) and hydrogen (H_2), supported by the X-ray rocking curve data.

In this article, we attempt to apply the modified four-step method to grow 3C–SiC on Si(111). The optimum experimental parameters are different from those used for the growth of 3C–SiC on Si(100) since the atomic arrangements in Si(111) and Si(100) are different [15]. The crystal quality of 3C–SiC on Si(111) is characterized. The effect of diffusion step on the growth of 3C–SiC on Si(111) is emphasized.

2. Experimental details

The experimental procedures for the growth of 3C–SiC(111) on Si (111) are similar to those used in our previous work [15] and are described in the following. 3C–SiC films were grown on off-axis 1.5° p-type Si(111) substrates by low pressure chemical vapor deposition (LPCVD). The LPCVD system is a horizontal type of a cold wall quartz tube that has been illustrated by other groups [16–18]. The Si(111) substrates were etched in a solution of 1% HF for 1 min in order to remove the native oxide and then rinsed with deionized water. The as-rinsed Si(111) substrates were put on a SiC coated graphite susceptor in

* Corresponding author. 101, Sec. II, Kuang-Fu Road, Hsin-Chu, Taiwan, ROC. Tel.: +886 3 5722577.
E-mail address: jch@mx.nthu.edu.tw (J. Hwang).

0040-6090/$ – see front matter © 2010 Elsevier B.V. All rights reserved.
doi:10.1016/j.tsf.2010.05.055

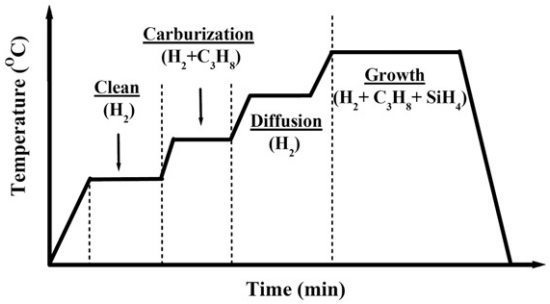

Fig. 1. Schematic showing the four-step (clean, carburization, diffusion, and growth) process for the growth of 3C–SiC on the 1.5° off-axis Si (111) towards [$\bar{1}$10].

Table 1
Optimum experimental parameters for the growth of high quality 3C–SiC films on Si (111) using the modified four-step process.

	Clean	Carburization	Diffusion	Growth
H_2 (sccm)	1000	1000	1000	1000
C_3H_8 (sccm)	0	11	0	3
SiH_4 (sccm)	0	0	0	20
Temperature (°C)	900	1250	1350	1395
Pressure (Torr)	10	2	2	0.8
Time (min)	5	1.5	5	30

the reactor. A mixed gas of C_3H_8 (99.99%) and SiH_4 (5% diluted in H_2) was carried by H_2 (99.999%) of 1 slm into the LPCVD system for the growth of 3C–SiC films at a base pressure of ~0.266 Pa. The substrate temperature was ramped up at the rate of 11 °C/s, monitored by either a thermocouple or an infrared pyrometer. The optimum experimental parameters of the modified four-step process for the growth of high quality of 3C–SiC films on Si(111) are tabulated in Table 1. The concentration of C_3H_8 in the carburization step and diffusion step are 1% and 0.3%, respectively. The carburization temperature should be high enough to dissociate C_3H_8. The optimum carburization temperature is 1250 °C, in such a condition the voids at the 3C–SiC/Si(111) interface can be minimized. The role of diffusion step is to transform the as-carburized layer fully into SiC by transporting Si atoms out of the Si(111) substrate at high temperature. The optimum diffusion temperature is 1350 °C.

The crystal qualities of 3C–SiC films were characterized using a Rigaku D/MAX2000 X-ray diffractometer (XRD) with Cu Kα radiation (1.545 Å) (operation voltage: 30 kV, currents: 20 mA) and a Philips TECNAI 20 Transmission Electron Microscope (TEM) (operation voltage: 200 kV). The 3C–SiC/Si(111) cross-sectional samples for TEM studies were prepared using a focused ion beam facility (FIB; FEI NOVA 200). The Ga^+ ions in FIB are accelerated and incident onto the 3C–SiC/Si (111) sample at various angles in preparation for TEM cross-sectional samples. The surface morphologies of 3C–SiC films were investigated by a JEOL JSM-6500F Field-Emission Scanning Electron Microscope (FESEM) operated at 15 kV. An X-ray photoemission spectroscopy (XPS; PHI ESCA 1600) was used to characterize the bonding characteristics of the grown 3C–SiC films. All the samples were slightly sputtered to clean their surfaces by Ar^+ ions before XPS measurements. C 1s spectra are plotted in a binding energy scale, which were excited using Mg Kα (1253.6 eV; 0.3 A/cm^2). The fitting software PeakFit was used to de-convolute the C 1s spectra using a Voigt function that is a Gaussian

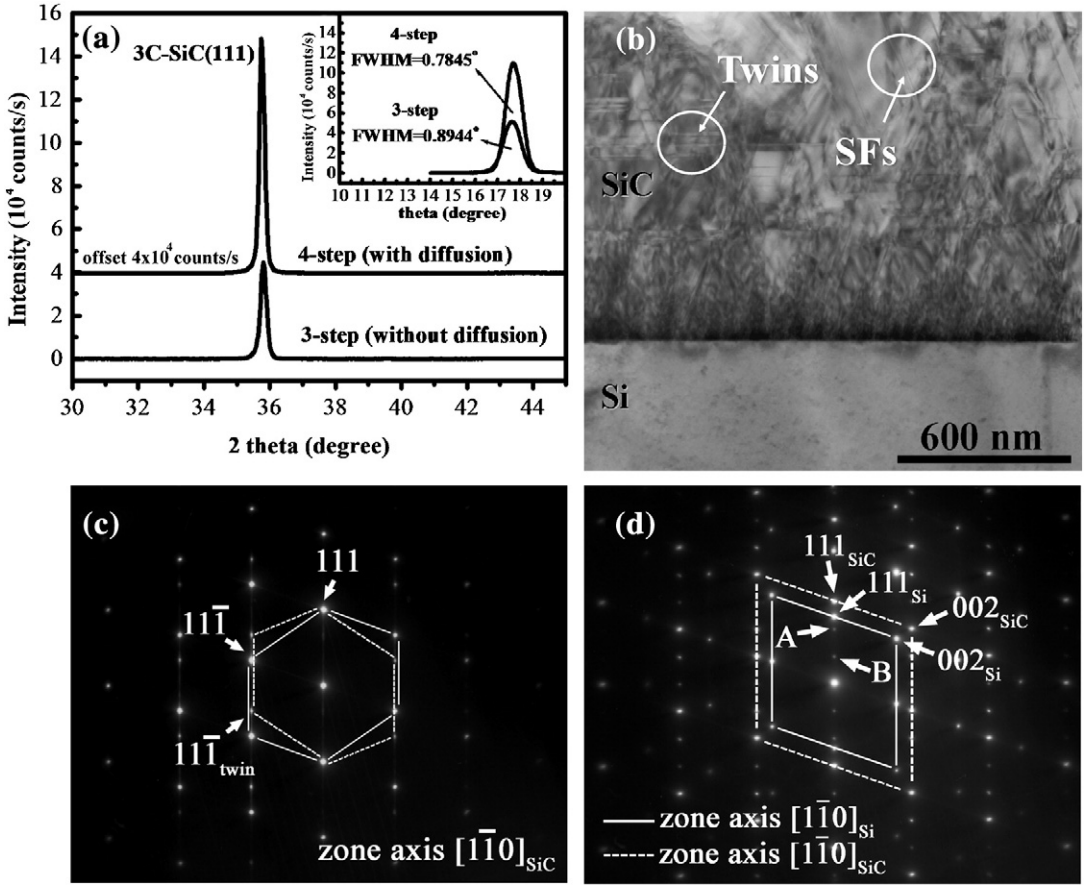

Fig. 2. (a) X-ray diffraction patterns of the 3C–SiC grown on the 1.5° off-axis Si(111) towards [$\bar{1}$10]. The prominent peak at $2\theta = 35.7°$ is diffracted from 3C–SiC (111). The X-ray rocking curve of 3C–SiC(111) is inserted in the upper-right corner. (b) Bright field image of the 3C–SiC/Si(111). There exist crystal defects such as stacking faults (SFs) and twins in the SiC layer near the interface. (c) The selective area electron diffraction (SAED) patterns of SiC film along the zone axis [$\bar{1}$10]. (d) The selective area electron diffraction (SAED) patterns of the 3C–SiC/Si(111) along the zone axis [$\bar{1}$10].

function convoluted with a Lorentzian function. The background function was represented in a power-law form. The C 1s peak widths of deconvoluted components are constrained to be the same in the peak fit analysis.

3. Results and discussion

Fig. 2a shows the XRD patterns of 3C–SiC films grown on the off-axis 1.5° Si(111) substrates using the three-step (without diffusion) and the modified four-step (with diffusion) methods. The three-step method is a modified three-step one consisting of three steps (clean, carburization and growth) without cooling between each step that is used for comparison. The diffracted peak at $2\theta = 35.7°$ is from the (111) plane of 3C–SiC according to the database of joint committee on powder diffraction standards (JCPDS). No other peaks corresponding to the (200) or (220) planes of 3C–SiC are detected, indicating that the as-grown 3C–SiC films are in either epitaxial (single crystalline) or highly oriented (textured) form [19]. The crystal quality of 3C–SiC is improved by adding the diffusion step since the (111) peak intensity of 3C–SiC increases from 5×10^4 counts/s (the modified three steps) to 1.1×10^5 counts/s (the modified four steps). The improvement of 3C–SiC crystal quality is further confirmed by the X-ray rocking curve of the (111) peak of 3C–SiC as shown in the inset of Fig. 2a. The full width at half maximum (FWHM) of 3C–SiC(111) reduces from 0.89 to 0.78 when the diffusion step is added. This supports that the crystal quality of 3C–SiC is improved by adding the diffusion step. In comparison with 3C–SiC film grown on Si(100) where the intensity of (200) plane at $2\theta = 41.5°$ is about 3×10^4 counts/s [15], the intensity of (111) plane of 3C–SiC grown on Si(111) is higher by about 2.7 times. This implies that the crystal quality of 3C–SiC on Si(111) is better than that on Si(100).

The crystal quality of 3C–SiC on Si(111) is further revealed in the bright field image taken at the 3C–SiC/Si(111) interface shown in Fig. 2b. There exist crystal defects such as stacking faults and twins in the 3C–SiC layer [6,8]. The selective area electron diffraction (SAED) pattern in Fig. 2c was taken from the 3C–SiC along the zone axis [$\bar{1}\bar{1}$0]. Two pairs of <111> type SAED spots are indexed to be twins of 3C–SiC. This is in good agreement with the observation of the twin image marked in the bright field image in Fig. 2b. The crystal orientations of SiC and Si at the interface can be revealed from the SAED pattern taken at the 3C–SiC/Si(111) interface along the zone axis [$\bar{1}$10]. The SAED spots in the SAED pattern are indexed in Fig. 2d, where the [111] (or [002]) spots of 3C–SiC are in parallel with those of Si. This supports that 3C–SiC[111] is lined up with Si[111]. In other words, 3C–SiC is epitaxially grown on Si(111). Note that some weak SAED spots arising from stacking faults (SFs) and twins marked with "A" and "B," respectively, also appear in Fig. 2d [9]. This agrees well with the observation of stacking faults and twins in the bright field image in Fig. 2b. The existence of twins and stacking faults implies the hetero-epitaxial layer of 3C–SiC on Si(111) is under stress due to large mismatch at the interface [20,21]. This can also explain why the crystal quality of 3C–SiC becomes better far away from the interface according to the bright field image.

The chemical bonding information in the as-carburized and as-diffused 3C–SiC layers can be extracted from the curve-fits of C 1s XPS spectra in Fig. 3a and b. Similar to the work of 3C–SiC on Si(100) [15], the C 1s curve of the as-carburized Si (111) (after the 2nd step) in Fig. 3a exhibits a prominent C–C and a Si–C component approximately at a binding energy of 284.5 eV and 283.2 eV, respectively. This indicates that not all the C–C bonds are transformed into Si–C bonds in the as-carburized layer at 1250 °C for 90 s during the carburization step. With the aid of the diffusion step at 1350 °C for 5 min, the C–C bonds greatly reduce associated with the increase of Si–C bonds, as clearly supported by the curve-fit result in Fig. 3b. Considering the SAED patterns taken from 3C–SiC and the 3C–SiC/Si(111) interface in Fig. 2c and d, both SiC is in a form of crystal. No crystalline structures other than SiC were detected in the SAED patterns. The C–C bonds

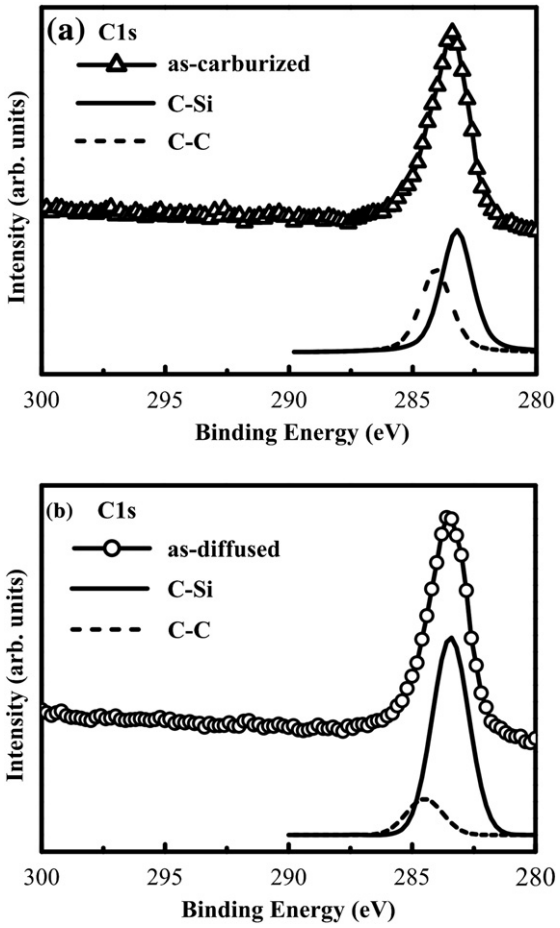

Fig. 3. C 1s XPS spectra of (a) as-carburized Si(111) (after the 2nd step) and (b) as-diffused 3C–SiC/Si(111) (after the 3rd step).

extracted from the curve-fit in Fig. 3 thus result from the residual carbon in a non-crystalline form, in good agreement with the results of Sun et al. [22]. The crystal quality of SiC in the as-diffused layer enables the growth of a SiC film of good crystal quality during the growth step (4th step). This is supported by the higher intensity and smaller FWHM of the 3C–SiC(111) peak in Fig. 2a.

The main difference in the growth of 3C–SiC on Si(111) and Si(100) is the easier formation of voids at the 3C–SiC/Si(111) interface. It has been proven that diffusion of Si atoms out of Si(111) occurs at a temperature higher than a critical temperature (approximately 850 °C) [13,23,24]. The carburization step is kept at approximately 1250 °C such that C_3H_8 can be decomposed and a large amount of carbon can be deposited onto Si(111) in order to form an ultra-thin SiC layer. The formation of voids at the 3C–SiC/Si(111) interface has been attributed to the out-diffusion of Si atoms during the formation of the ultra-thin SiC layer at the carburization step [10,23–25]. Fig. 4a and b are the SEM images showing the voids at the 3C–SiC/Si(111) interfaces prepared by the three-step (without diffusion) and the modified four-step (with diffusion) methods, respectively. Voids of 0.2–0.5 μm in width and ~0.2 μm in depth reside at both interfaces as shown in the insets in Fig. 4a and b. The density of voids becomes less at the 3C–SiC/Si(111) interface prepared by the modified four-step method. This indicates that the diffusion step can reduce the density of voids. The void formation has been attributed to the out-diffusion of Si atoms at the carburization step in previous publications [10,23–25]. If the void formation were completed at the carburization step, the diffusion step at higher temperature (1350 °C) would not affect the density of voids. However, it is not the case. The reduction of void density in the modified four-step method can be well explained by the incomplete void formation at the

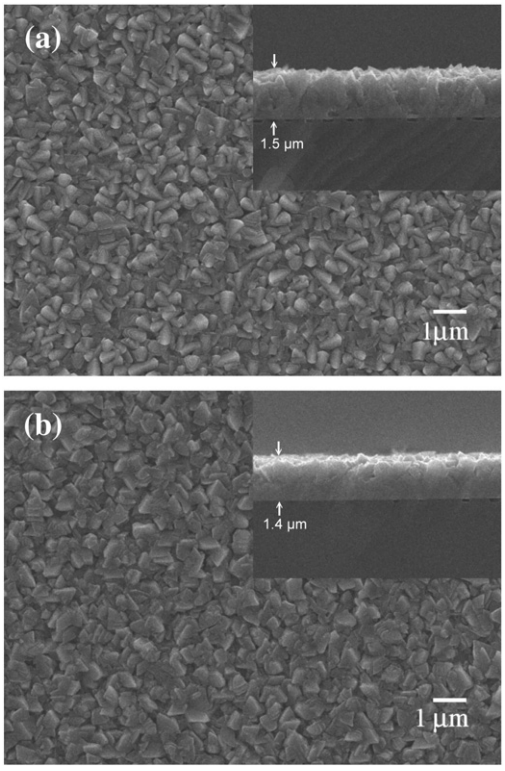

Fig. 4. SEM images showing the morphologies of 3C–SiC films grown on the off-axis 1.5° Si (111) towards [$\bar{1}$10] under different growth conditions: (a) 3 steps (without diffusion) and (b) 4 steps (with diffusion). The cross-sectional view SEM images are inserted in the upper-right corners.

carburization step. In the three-step method, voids continue to form at the 3C–SiC/Si(111) interface during the growth step at 1395 °C. The diffusion step, in the modified four-step method, plays a major role in enhancing the formation of Si–C bonds and also a minor role in reducing the void formation due to lower temperature (1350 °C). The argument above and the data in Fig. 4b thus support that void formation is not completed at the carburization step. The temperature at the diffusion step is lower than that at the growth step, which is the physical reason for the reduction of density of voids.

4. Conclusions

A high quality of 3C–SiC can be grown on Si(111) using the modified four-step method in LPCVD. The optimum experimental parameters for the growth of 3C–SiC on Si(111) are different from those on Si(100). The diffusion step followed by the carburization step can transform most residual C–C bonds into the Si–C bonds in the as-carburized layer. The formation of Si–C bonds helps the epitaxial growth of 3C–SiC on Si(111) at the growth step. The diffusion step also reduces the void density at the 3C–SiC/Si(111) interface. However, stacking faults and twins are generated near the 3C–SiC/Si(111) interface due to large lattice mismatch.

References

[1] J.B. Casady, R.W. Johnson, Solid-State Electron. 39 (1996) 1409.
[2] J.A. Cooper, S. Yoshida, S. Nishino, H. Harima, T. Kimoto, Mater. Sci. Forum 389–393 (2002) 15.
[3] C.E. Weitzel, J.W. Palmour, C.H. Carter, K. Moore, K.J. Nordquist, S. Allen, C. Thero, M. Bhatnagar, IEEE Trans. Electron. Devices 43 (1996) 1732.
[4] S. Nishino, J.A. Powell, H.A. Will, Appl. Phys. Lett. 42 (1983) 460.
[5] H. Nagasawa, K. Yagi, Phys. Status Solidi B 202 (1997) 335.
[6] M.J. Hernandez, G. Ferro, T. Chassagne, J. Dazord, Y. Monteil, J. Cryst. Growth 253 (2003) 95.
[7] Y. Ishida, T. Takahashi, H. Okumura, S. Yoshida, J. Appl. Phys. 94 (2003) 4676.
[8] H. Nagasawa, K. Yagi, T. Kawahara, N. Hatta, Chem. Vap. Depos. 12 (2006) 502.
[9] F.M. Morales, S.I. Molina, D. Araujo, R. García, V. Cimalla, J. Pezoldt, Diam. Relat. Mater. 12 (2003) 1227.
[10] J.P. Li, A.J. Steckl, J. Electrochem. Soc. 142 (1995) 634.
[11] A.J. Steckl, J.P. Li, IEEE Trans. Electron. Devices 39 (1992) 64.
[12] A. Severino, G. D'Arrigo, C. Bongiorno, S. Scalese, F. La Via, G. Foti, J. Appl. Phys. 102 (2007) 10.
[13] K. Ikoma, M. Yamanaka, H. Yamaguchi, Y. Shichi, J. Electrochem. Soc. 138 (1991) 3028.
[14] P. Liaw, R.F. Davis, J. Electrochem. Soc. 132 (1985) 642.
[15] W.Y. Chen, C.C. Chen, J. Hwang, C.F. Huang, Cryst. Growth Design 9 (2009) 2616.
[16] S. Nishino, Y. Hazuki, H. Matsunami, T. Tanaka, J. Electrochem. Soc. 127 (1980) 2674.
[17] M.I. Chaudhry, R.L. Wright, J. Mater. Res. 5 (1992) 1595.
[18] Y. Ishida, T. Takahashi, H. Okumura, S. Yoshida, T. Sekigawa, Jpn. J. Appl. Phys. 36 (1997) 6633.
[19] A.J. Steckl, C. Yuan, J.P. Li, M.J. Loboda, Appl. Phys. Lett. 63 (1993) 3347.
[20] U. Kaiser, S.B. Newcomb, W.M. Stobbs, M. Adamik, A. Fissel, W. Richter, J. Mater. Res. 13 (1998) 3571.
[21] M.A. Capano, B.C. Kim, A.R. Smith, E.P. Kvam, S. Tsoi, A.K. Ramdas, J. Appl. Phys. 100 (2006) 3.
[22] Y. Sun, T. Miyasato, N. Sonoda, J. Appl. Phys. 84 (1998) 6451.
[23] J. Jinschek, U. Kaiser, W. Richter, Mater. Sci. Forum 338 (2000) 521.
[24] Y.H. Seo, K.C. Kim, H.W. Shim, K.S. Nahm, E.K. Suh, H.J. Lee, D.K. Kim, B.T. Lee, J. Electrochem. Soc. 145 (1998) 292.
[25] A. Gupta, J. Sengupta, C. Jacob, Thin Solid Films 516 (2008) 1669.